Model Predictive Control Strategy for Residential Battery Energy Storage System in Volatile Electricity Market with Uncertain Daily Cycling Load

Dejan P. Jovanović, Gerard F. Ledwich, and Geoffrey R. Walker

***Abstract*—This paper presents a control strategy for residential battery energy storage systems, which is aware of volatile electricity markets and uncertain daily cycling loads. The economic benefits of energy trading for prosumers are achieved through a novel modification of a conventional model predictive control (MPC). The proposed control strategy guarantees an optimal global solution for the applied control action. A new cost function is introduced to model the effects of volatility on customer benefits more effectively. Specifically, the newly presented cost function models a probabilistic relation between the power exchanged with the grid, the net load, and the electricity market. The probabilistic calculation of the cost function shows the dependence on the mathematical expectation of market price and net load. Computational techniques for calculating this value are presented. The proposed strategy differs from the stochastic and robust MPC in that the cost is calculated across the market price and net load variations rather than across model constraints and parameter variations.**

***Index Terms*—Optimal control, model predictive control (MPC), energy market, nonlinear constrained optimization, revenue for battery energy storage system, Gaussian mixture model, autoregressive integrated moving average model.**

I. Introduction

THE promising economic benefits of battery energy storage systems (BESSs) for residential customers [1] offer many investment opportunities [2]. Investment assets include BESSs and equipment for renewable energy generation. Risks associated with these assets are mainly related to how well electricity market price spikes are managed [3], [4]. Market price spikes are defined as price jumps of extreme size due to sudden imbalances in supply and demand [5]. The situation is similar to power network generators, which generate most of the revenue during market price spikes [3], [6]. To take advantage of investment opportunities, a proper control strategy is required to evaluate the revenue and net income [7]. A control strategy for residential customers requires that storage volumes, net load characteristics, and market price [8], [9] are all considered and that globally optimal decisions are made.

The control strategy often used for a BESS control is model predictive control (MPC), which is a cost-minimizing iterative optimization method over a finite prediction horizon [10]. Numerous studies on MPC and its application in BESS control have been conducted. In [11], an MPC-based approach is proposed to optimize energy costs to the end-user. In this approach, a two-stage strategy is developed to separate the BESS control action between the energy deficit and excess. The load volatility is suppressed by introducing weights assigned to the cost of output error. Through this approach, customer benefits are significantly reduced. Inequality constraints are not imposed on a BESS. The concept of an end-user-driven microgrid is introduced in [12]. In this strategy, end-users can consume and share power only with the utility grid. A dynamic MPC-based optimization approach is used for the optimal power and battery scheduling. A constant demand and very low load volatility are assumed. Reference [13] considers a rule-based MPC controller in which rules are based on the operating constraints of the BESS. The BESS control is defined as an optimal tracking problem, whereas the reference inputs are assumed to have a smooth trajectory. The methodology proposed in [14] combines an MPC with a Gaussian process based prediction for photovoltaic (PV) generation and demand. The study determines that a shorter MPC horizon provides more accurate control. Here, the prediction method outperforms the rule-based MPC algorithm. In [15], the distributed and decentralized MPC of a residential BESS is designed, in which the load variability is flattened using averaging over the receding horizon, and terminal constraints are not considered. A mixed-integer multi-time scale stochastic optimization based on an MPC is proposed in [16] for home energy management. Here, the cost function is minimized (subject to bud-

Manuscript received: March 30, 2021; revised: August 10, 2021; accepted: November 12, 2021. Date of CrossCheck: November 12, 2021. Date of online publication: March 2, 2022.

This work was supported by Australian Research Council (ARC) Discovery Project (No. 160102571).

D. P. Jovanović (corresponding anthor) is with Institute of Electrical and Electronic Engineers, Queensland, Australia (e-mail: jovanovd@ieee.org).

G. F. Ledwich and G. R. Walker are with the School of Electrical Engineering & Robotics, Queensland University of Technology, Brisbane, Australia (e-mail: g.ledwich@qut.edu.au; geoffrey.walker@qut.edu.au).

DOI: 10.35833/MPCE.2021.000207

get and power constraints) such that the indoor temperature is maintained at the reference level. The electricity price is assumed to be constant, and the load has a low variability.

Electrical energy trading is rapidly changing with the increase in distributed energy resource (DER) connections. Traditional energy consumers are becoming prosumers that both consume and generate energy [17]. In essence, the electricity generation of DERs is challenging to predict because of the stochastic nature of these resources. However, if energy is stored in a BESS and exported back to either the grid or other energy consumers, the optimal BESS control can achieve economic benefits. The volatility of the electricity market price and uncertain cycling load mean that finding an optimal solution for a customer BESS is challenging. Market price involves a nonlinear stochastic process that consists of the base price and spikes [5]. Therefore, the price characterization is a demanding but vital task [4], as managing market price spikes is critical in mitigating the risks of investing in BESSs for residential customers.

In this context, MPC must address the following challenges. First, the control strategy must be optimal. The conventional MPC does not guarantee optimality. Furthermore, the daily repetitive nature of the net load causes the receding one-day-ahead prediction horizon of the MPC to have different levels of cycling load. Consequently, the equality terminal constraint becomes too challenging to incorporate into the optimization process. The final challenge is modelling the probabilistic characterization of energy prices and incorporating them into the MPC.

To achieve the optimal economic benefits for customers in a volatile electricity market with a daily cycling load, we propose a control strategy based on a modified version of a conventional MPC. A new cost function is proposed that models a probabilistic relation between flow, the net load, and the electricity market. We show that this cost function is convex and applicable to convex optimization. The numerical quantification of the proposed cost function is based on calculations of expected values of the market price and net load. The variable length horizon is introduced, which enables the equality terminal constraint to be defined at a time of low power. The computational techniques for calculating the expected values are proposed for a volatile market price and daily cycling load. An innovative application of a mixture model for calculating the expected value of a volatile market price is introduced. The proposed optimization method is convex and guarantees a globally optimal solution. Finally, because the model of a household equipped with a BESS is a linear time-varying switching one (as it depends on the energy flow direction), we propose a strategy that directly incorporates a switching model in the cost function.

The remainder of this paper is organized as follows. In Section II, the BESS modelling is described. Section III describes progressive MPC for volatile electricity market price and cycling daily load. The calculation of the expected values of the market price is addressed in Section IV. The results are presented in Section V and the conclusions are given in Section VI.

II. BESS Modelling

The subsystems that comprise a BESS system include a control unit, communication link, and smart meter. The control unit regulates the energy stored in the batteries driven by a variable local demand and energy price. The communication link is assumed, through which the information about energy price changes is provided to the control unit in real time. A smart meter measures the energy flow between the power grid and a household equipped with a BESS. A simplified block of a household equipped with a BESS is presented in Fig. 1, where $F(t)$ is the power exchanged with the grid and measured by the smart meter; $L(t)$ is the net load power defined as the difference between local demand and local generation; and $u(t)$ is the battery power.

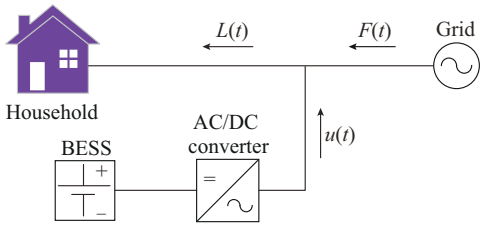

Fig. 1. Simplified block of a household equipped with a BESS.

The energy capacity of the BESS is given by E_c. The realistic modelling of the battery charging and discharging processes requires realistic values for charging losses α^- and discharging losses α^+. The charging process is assumed to be less efficient than the discharging process [18], [19]. Based on these characteristics, a state space model of a proposed grid-connected BESS is given by:

$$E_{t+1} = E_t - \bar{\alpha} u_t \Delta T \tag{1}$$

where $\bar{\alpha}$ is the loss term; E_t and E_{t+1} are the instantaneous battery energy at time instance t and $t+1$, respectively; and ΔT is the time interval. $\bar{\alpha}$ is defined as:

$$\bar{\alpha} = \begin{cases} \alpha^+ & u_t > 0 \\ \alpha^- & u_t \le 0 \end{cases} \tag{2}$$

In this paper, losses in a battery are defined as a function of inverter efficiency because mapping all losses to the DC side of an inverter is possible [13]. The state of charge (SOC) of a battery system is modelled by:

$$SOC_{t+1} = SOC_t - \frac{\bar{\alpha} u_t \Delta T}{E_c} \tag{3}$$

where SOC_t and SOC_{t+1} are the SOCs of a battery at time instance t and $t+1$, respectively.

Complex battery models [19], [20] are not used in this study because they do not affect the overall design process.

Constraints are imposed on the control input u_t, requiring that:

$$-P_c \le u_t \le P_c \tag{4}$$

where P_c is the maximum power rating of the converter.

In addition, the minimum and maximum BESS energy levels impose constraints on acceptable values of instantaneous energy such that the following relations hold:

$$E_{res} \le E_{t+1} \le E_c \tag{5}$$

where E_{res} is the contracted level of energy reserve. Finally, the constraint that ensures that the BESS energy level at the end of the time horizon has the predefined value E_{end} as:

$$E_{t_H} = E_{end} \tag{6}$$

where E_{t_H} is the equality terminal constraint. It follows that the underlying model of the system shown in Fig. 1 is a linear time-varying switching model because (1) depends on the energy flow direction. Subsequently, the control of BESS is a time-varying nonlinear control problem. In addition to nonlinearity, a control problem of BESS is constrained with a set of operational limitations given by (4)-(6).

The flow balance of the system shown in Fig. 1 is disrupted by cycling random dynamics of the household net load. However, the economic benefits of a household are determined by market price. Incorporating these dynamics in the control methodology and evaluating the cost across the net load variability and market price are essential.

III. Progressive MPC for Volatile Electricity Market Price and Cycling Daily Load

MPC on the finite horizon $[t_1, t_H]$ is defined as a convex optimization problem by:

$$\begin{cases} \min\limits_{\boldsymbol{u}} C(\boldsymbol{u}) \\ \text{s.t. } \varphi_i(\boldsymbol{u}) \le 0 \quad \varphi_i: \mathbb{R}^H \mapsto \mathbb{R},\ i = 1, 2, ..., l \\ \quad\ \psi_j(\boldsymbol{u}) = 0 \quad \psi_j: \mathbb{R}^H \mapsto \mathbb{R},\ j = 1, 2, ..., m \end{cases} \tag{7}$$

where $C(\boldsymbol{u})$ is the cost function and $\boldsymbol{u} \in \mathbb{R}^H$ is the optimization control variable. The functions $C(\cdot)$ and $\varphi_i(\cdot)$ are convex, whereas the function $\psi_j(\cdot)$ is affine [6]. Since (1) is the forward difference approximation of the first derivative, it follows that nonlinear constraint (5) is convex [22]. The equality constraint (6) is affine for the finite horizon $[t_1, t_H]$, since (1) can be re-written as an affine transformation in the following form:

$$\Phi(\boldsymbol{u}) = \boldsymbol{A}\boldsymbol{u} + \boldsymbol{b} \tag{8}$$

where $\Phi(\cdot)$ is the cumulative distribution function (CDF) of the standard normal distribution; $\boldsymbol{A} = -\text{diag}[\Delta T, \Delta T, ..., \Delta T]_{H \times H}$ is a linear transformation; $\boldsymbol{u} = [\bar{\alpha} u_1, \bar{\alpha} u_2, ..., \bar{\alpha} u_H]^{\mathrm{T}}$; and $\boldsymbol{b} = [E_{t_1}, E_{t_2}, ..., E_{t_H}]^{\mathrm{T}}$. It is worth noting that on the finite horizon $[t_0, t_H]$, E_{t_H} at a fixed-end horizon time t_H can be written as:

$$E_{t_H} = E_{t_0} - \sum_{\tau=t_0}^{t_{H-1}} \bar{\alpha} u_\tau \Delta T \tag{9}$$

where τ is a discrete-time step at which the total cost is computed.

With the constraints satisfying the convex optimization conditions, it remains to prove that the cost function is also convex. Before proving the convex optimization property, we first introduce the new cost function and the assumptions upon which this function rests.

The total cost of the BESS response to market price over time interval $t \in [t_0, t_H]$ is modelled as:

$$C_{tot} = \int_{t_0}^{t_H} g(M(t), F(t)) \mathrm{d}t \tag{10}$$

where $g(M(t), F(t))$ is the instantaneous cost, which depends on the market price and power exchanged with the power grid; and $M(t)$ is the market price.

The framework upon which the integrand $g(M(t), F(t))$ is defined is based on the assumption that flow $F(t)$ cannot influence $M(t)$ because of the limited and insufficient energy capacity of the household BESS. In addition, because the individual household is not the relevant entity in the bidding process, no mechanism exists for the energy market to influence the particular household flow directly. Consequently, the instantaneous cost definition can be given in the following form:

$$g(M(t), F(t)) = M(t)F(t) \tag{11}$$

Since the random nature of $M(t)$ and $F(t)$, the total cost (10) must be calculated as the expected value. Applying the operator of the mathematical expectation to (10), the expected total cost is given by:

$$\mathbb{J} = \mathbb{E}\{C_{tot}\} = \mathbb{E}\left\{\int_{t_0}^{t_H} g(M(t), F(t)) \mathrm{d}t\right\} \tag{12}$$

Interchanging the integral with mathematical expectation is possible if and only if an integrand $g(M, F)$, where M and F are random variables, is bounded [23]. This condition is satisfied since all variables in $g(M, F)$ are constrained by their maximum values. After the integral is interchanged with mathematical expectation and is approximated with a sum, (12) becomes:

$$\mathbb{J} = \mathbb{E}\{C_{tot}\} = \sum_{\tau=0}^{H} \mathbb{E}\left\{g_\tau(M, F)\right\} \Delta T \tag{13}$$

A computation of total cost is reduced to a computation of the expected value of a function $g_\tau(M, F)$ for τ. The battery action is assumed to be fixed for each evaluation. By definition, the expected value of a function $g_\tau(M, F)$ is given by:

$$\mathbb{E}\left\{g_\tau(M, F)\right\} = \iint_{M,F} g_\tau(m, f) p_{M,F}(m, f) \mathrm{d}m \mathrm{d}f \tag{14}$$

where $p_{M,F}(m, f)$ is the joint probability density function (PDF) [5], [24]; and M and F are considered independent in terms of the calculation of (14). Consequently, $p_{M,F}(m, f)$ is a product of two univariate PDFs $p_M(m)$ and $p_F(f)$.

$$p_{M,F}(m, f) = p_M(m) p_F(f) \tag{15}$$

Substituting (11) and (15) into (14) yields the expectation in its unfolded form as:

$$\mathbb{E}\left\{g_\tau(M, F)\right\} = \int_{-\infty}^{\infty} m p_M(m) \mathrm{d}m \int_{-\infty}^{\infty} f p_F(f) \mathrm{d}f \tag{16}$$

Previous studies on electricity spot price show that market price consists of two components: base price and spikes [5], [6], [25], [26]. The base price component represents the daily fluctuations of the price around the mean level, whereas spikes are the price jumps of extreme size due to a sudden imbalance of supply and demand [5]. Based on these findings, the dynamic range of the market price in (16) can be given by the following relation $M = \bar{M} \cup \tilde{M}$. M is represented as the union of two clusters $\bar{M}$ (the base component of the market price) and $\tilde{M}$ (the non-predictable market price spike component). In [27], it is proven that each cluster can be modelled as a random variable. Consequently, M is modeled

as a mixture of $\bar{M}$ and $\tilde{M}$, defined as:

$$M=\bar{M}\mathbb{I}_{\bar{M}=M}+\tilde{M}\mathbb{I}_{\tilde{M}=M} \tag{17}$$

where $\mathbb{I}_{\bar{M}=M}$ and $\mathbb{I}_{\tilde{M}=M}$ are the latent variables [28] used to specify the identity of the mixture component of each observation M. Consequently, the market price PDF can be written as:

$$p_M(m)=(1-\gamma)p_{\bar{M}}(m)+\gamma p_{\tilde{M}}(m) \tag{18}$$

where γ is the PDF weight and takes the value $0<\gamma<1$. Substituting (18) into (16) yields the expected value of the instantaneous cost as:

$$\mathbb{E}\{g(M,F)\}=\left[(1-\gamma)\int_{-\infty}^{\infty}mp_{\bar{M}}(m)\mathrm{d}m+\gamma\int_{-\infty}^{\infty}mp_{\tilde{M}}(m)\mathrm{d}m\right]\int_{-\infty}^{\infty}fp_F(f)\mathrm{d}f \tag{19}$$

The compact form of (19) is given as:

$$\mathbb{E}\{g_\tau(M,F)\}=(\mathbb{E}\{\bar{M}\}+\mathbb{E}\{\tilde{M}\})\mathbb{E}\{F\} \tag{20}$$

The result from (20) is of two-fold importance. First, it demonstrates that the calculation of the expected cost is reduced to the calculation of the expected values of both the energy market price and the power exchanged with the grid. Second, it can be used to prove the convexity of the optimization problem. When (10) is used in a convex optimization, it is required to prove that it is convex. The first step is to prove that (11) is convex. The following proof is based on the results in [29], where a converse of Jensen's inequality is shown. Assuming the existence of closed convex sets and a continuous probabilistic measure, the converse of Jensen's inequality holds [29].

Theorem 1: an instantaneous cost (11) is a convex function.

Proof: it follows from (19) that γ determines the ratio between $\bar{M}$ and $\tilde{M}$. Since the market price spike component can be considered as rare even with a low probability, it is possible to assume that $\gamma\ll1-\gamma$ and $\mathbb{E}\{\bar{M}\}\approx\mathbb{E}\{M\}$; then $\mathbb{E}\{\bar{M}\}+\mathbb{E}\{\tilde{M}\}$ represents the upper boundary of expected market price. Consequently, the following inequality can be obtained.

$$\mathbb{E}\{g_\tau(M,F)\}=\left(\mathbb{E}\{\bar{M}\}+\mathbb{E}\{\tilde{M}\}\right)\mathbb{E}\{F\}\geq\mathbb{E}\{M\}\mathbb{E}\{F\} \tag{21}$$

Since $M,\bar{M},\tilde{M}\in\mathbb{R}$, they represent closed convex sets. In addition, their PDFs are assumed to be absolutely continuous. Based on these assumptions as well as the inequality (21) and results from [29], it follows that (11) is a convex function.

According to the theorem of calculus [22], which states that the integral of a convex function is also convex, and Theorem 1, it follows that the integral (10) is a convex function. Therefore, it follows that the proposed MPC strategy is a convex optimization problem that guarantees that every local minimum is a global minimum [22].

To calculate the expected value of flow $\mathbb{E}\{F\}$, $F(t)$ is a function of $L(t)$ and $u(t)$, as shown in Fig. 1. Modelling of time dependence in the MPC requires that two time scales should be introduced, i. e., time instance t and simulation time index k. Consequently, the time-dependent flow balance shown in Fig. 1 is given by:

$$F_{k|t}=L_{k|t}-u_{k|t} \tag{22}$$

where $F_{k|t}$ is the power flow; $L_{k|t}$ is the load; and $u_{k|t}$ is the battery power and is deterministic since it is a result of the MPC algorithm from a previous time instance $t-1$ when the integral (19) is calculated. Note that $F_{k|t}$ and $L_{k|t}$ are random variables. A change of the variables in (22) to the expression for the expectation $\mathbb{E}\{F\}$ yields:

$$\mathbb{E}\{F\}=\int_{-\infty}^{\infty}f_{k|t}p_F(f_{k|t})\mathrm{d}f_{t,k}=\int_{-\infty}^{\infty}(l_{k|t}-u_{k|t})p_F(l_{k|t}-u_{k|t})\mathrm{d}f_{k|t} \tag{23}$$

where $f_{k|t}$ is the realization of $F_{k|t}$; and $l_{k|t}$ is the realization of $L_{k|t}$. Note that the subscript $k|t$ is the conventional MPC syntax for t and k. Sometimes, the subscript $k|t$ will be omitted.

Based on (22), a relation between the CDFs $\Phi_L(\cdot)$ and $\Phi_F(\cdot)$ must be modelled. The CDF of a real-valued random variable X is $\Phi_X(x)=P(X\leq x)$ [30]. Consequently, a relation between CDFs is given as:

$$\Phi_L(L)=P(L\leq l)=P(F+u\leq l)=P(F\leq l-u)=\Phi_L(l-u) \tag{24}$$

From (24), it follows that $p_L(l)\mathrm{d}l=p_F(l-u)\mathrm{d}f$, and from (22), it follows that $\mathrm{d}l=\mathrm{d}f$. Consequently, the expected flow is:

$$\mathbb{E}\{F\}=\int_{-\infty}^{\infty}(l_{k|t}-u_{k|t})p_L(l_{k|t})\mathrm{d}L_{k|t}=\int_{-\infty}^{\infty}l_{k|t}p_L(l_{k|t})\mathrm{d}l_{k,t}-u_{k|t}\int_{-\infty}^{\infty}p_L(l_{k|t})\mathrm{d}l_{k|t}=\mathbb{E}_{u_{k|t}}\{L\}-u_{k|t} \tag{25}$$

where $\mathbb{E}_{u_{k|t}}\{L\}$ is calculated as:

$$\mathbb{E}_{u_{k|t}}\{L\}=\int_{-\infty}^{\infty}l_{k|t}p_L(l_{k|t})\mathrm{d}l_{k|t} \tag{26}$$

The PDF $p_L(l_{k|t})$ satisfies the normalization condition $\int_{-\infty}^{\infty}p_L(l_{k|t})\mathrm{d}l_{k|t}=1$.

To compute the expected value (26) with an arbitrary load PDF $p_L(l_{k|t})$, Markov chain Monte Carlo (MCMC) [31] methods can be used. However, for computational simplicity, a random load is modelled with a Gaussian distribution $L_{k|t}\sim\mathcal{N}(\mu_{k|t},\sigma_{k|t}^2)$, where the mean value $\mu_{k|t}=\mathbb{E}_{u_{k|t}}\{L\}$ is the average daily load at any time point, and $\sigma_{k|t}^2$ is the constant load variation.

Since the expectations of the base and spike components in (20) are calculated with respect to t and k, their notations must be changed to $\mathbb{E}_{u_{k|t}}\{\bar{M}\}$ and $\mathbb{E}_{u_{k|t}}\{\tilde{M}\}$, respectively, to reflect the time dependence. Furthermore, it follows that when $k>1$ at time t, the expected values are computed as predictions $\mathbb{E}_{u_{k|t}}\{\bar{M}\}=\hat{\bar{M}}_{k|t}$, which are generated by an autoregressive integrated moving average (ARIMA) [32] model. For $k=1$, the expected value of the base price is equal to the observed market price at time instance t, $\mathbb{E}_{u_{1|t}}\{\bar{M}\}=M_t$. The spike expected value $\mathbb{E}_{u_{k|t}}\{\tilde{M}\}$ is calculated using a mixture model [28]. Details of the calculation of the expected values are provided in the following section.

In a conventional MPC [10], at each time instance, the end of the horizon is shifted toward the future. The resulting

control sequence is bounded by a set of constraints, both inequality and equality. One of the limitations of applying equality constraints to a conventional MPC for daily cycling load control is that the value of the end of the horizon affects the control sequence. Since the horizon passes through intervals with different values of load imbalance, it follows that the control sequence will depend on the load value at the end of the horizon. However, in the case of a household equipped with a BESS, given the cycling nature of the load, a different strategy is required. Compared with a conventional MPC, the proposed modified MPC strategy assumes that the end of the horizon is fixed and finishes at a time of low power. This assumption is justified by the fact that the load profile, on average, has a 24-hour recurrent interval. Consequently, the battery usage is predominantly defined by the morning and evening peaks; whereas after the evening peak, the battery usage is less demanding. In this manner, the horizon decreases while progressing toward the end of a recurrent interval. This control strategy is called progressive MPC (pMPC) since the horizon duration is variable and finally stops at a low demand by battery.

Once the load and market price are predicted, the values obtained are used in Algorithm 1 to calculate the pMPC sequence at time instance t on the finite horizon H.

Algorithm 1: pMPC

Step 1: start procedure: pMPC $(u_{k|t})_{k=1}^{H}$ and $(\hat{\mu}_{L_{k|t}}, \hat{\sigma}_{L_{k|t}})_{k=1}^{H}$

Step 2: $\mathbb{E}\{g_{k|t}(M,F)\}=\left(\mathbb{E}_{u_{k|t}}\{\bar{M}\}+\mathbb{E}_{u_{k|t}}\{\tilde{M}\}\right)\mathbb{E}_{u_{k|t}}\{F\}$

Step 3: $\mathbb{E}\{C_{tot}\}=\mathbb{E}_{u_{k|t}}\sum_{k=1}^{H} g_{k|t}(M,F)\Delta T-\lambda u_{k|t}\mathbb{I}_{u_{k|t}<0}$

Step 4: $\min_{u_{1|t+1}, u_{2|t+1}, ..., u_{H|t+1}} \mathbb{E}\{C_{tot}\}$

Step 5: return $u_{1|t+1}$

Step 6: end procedure

In *Step 1*, the input values are provided for the length of horizon H, the control sequence from the previous time step t, and the load PDF parameters $\hat{\mu}_{L_{k|t}}$, and corresponding variance $\hat{\sigma}_{L_{k|t}}$. The PDF parameters are used to calculate the expected load value $\mathbb{E}_{u_{k|t}}\{F\}$ in *Step 2*. In the same step, the expected values of the base price $\mathbb{E}_{u_{k|t}}\{\bar{M}\}$ and the spike expected value $\mathbb{E}_{u_{k|t}}\{\tilde{M}\}$ are calculated. It should be noted that for $k=1$, the expected value of the base price is equal to the observed market price at time instance t: $\mathbb{E}_{u_{1|t}}\{\bar{M}\}=M_t$. The remaining predicted values are generated by the ARIMA model. $\mathbb{E}_{u_{k|t}}\{\tilde{M}\}$ for each $k=1,2,...,H$ is obtained from mixture models described by a tuple of parameters $(\alpha_n, \mu_n, \sigma_n)$, $n \in K$, where α_n is the weighting coefficient of a component n; μ_n is the mean value of a component n; σ_n is the variance of a component n; and K is the number of components. As outlined in the introduction, to increase the battery life, penalizing the inflow variability is crucial. To achieve this, the expected cost function (13) is extended by adding a penalty term $-\lambda u_{k|t}\mathbb{I}_{u_{k|t}<0}$ for inflows, where λ is a weighting factor and the negative sign is positive for the penalty term. As a result, the control sequence $u_{1|t+1}, u_{2|t+1}, ..., u_{H|t+1}$ is calculated. As with the conventional MPC [10], from the sequence obtained, only the first control signal $u_{1|t+1}$ is used by the battery controller.

IV. Computation of Expected Values of Market Price

To calculate the expected values, the concept of the market price as the union of two clusters is discussed in the previous section. The first cluster is the base price and represents the daily fluctuations of the price near the mean level. The second cluster contains the price jumps of extreme size. These jumps represent outliers since they differ significantly from the base [5]. It follows that removing outliers [33] from the historical market price data creates the base price dataset, whereas outliers themselves create the market price spike dataset [6], [25], [34]. With the knowledge of the total number of data samples N and the number of data samples that are detected as outliers M, the coefficient γ in (18) is estimated as the ratio $\gamma = M/N$.

A. Expectation of Base Price Component

Since the energy price has a component with an approximately 24-hour period, daily varying ARIMA parameters (p, d, q) and a periodic differencing filter are proposed for the base energy price prediction model [35]. Once an ARIMA prediction is obtained, the expected value used in pMPC becomes $\mathbb{E}_{u_{k|t}}\{\bar{M}\}=\hat{\bar{M}}_{k|t}$. The results of the base price modelling are presented in Section V.

B. Expectation of Price Spike Component

Based on the historical data, the market price spike dataset is created as the set of market price outliers. Each time slot contains heterogeneous data. To model data within each time slot, it is proposed that a mixture of Gaussian distributions is modelled [28], each mixture component of which has a constant mean value and variance. This type of model is defined as:

$$F(\tilde{m}_t;\Theta)=\sum_{n=1}^{K}\alpha_k\Phi\left(\frac{\tilde{m}_t-\mu_n}{\sigma_n}\right) \tag{27}$$

where $F(\tilde{m}_t;\Theta)$ is the parametric CDF of the observation $\tilde{m}_t$ at time instance t; and α_k is a mixture weighting coefficient.

The mathematical expectation and variance can be expressed as a set of the following equations [28]:

$$\mathbb{E}\{\tilde{M}\}=\sum_{n=1}^{K}\alpha_n\mu_n \tag{28}$$

$$Cov\{\tilde{M}\}=\sum_{n=1}^{K}\alpha_n\left(\sigma_n+\mu_n\mu_n^{\mathrm{T}}\right)-\mathbb{E}\{\tilde{M}\}\mathbb{E}\{\tilde{M}\}^{\mathrm{T}} \tag{29}$$

To determine the number of clusters in practice, the Bayesian information criterion (BIC) [28] is commonly used.

In summary, each time slot is modelled using (27), and the corresponding expected value $\mathbb{E}_{u_{k|t}}\{\tilde{M}\}$ is given by (28). Once the expected values are estimated, pMPC is executed. It should be noted that, unlike the expected value of base price, which updates at each time instance, the expected value of market price spike is determined based on historical

data and does not change during operation.

V. Results

Simulation results are divided into three subsections. The first two subsections present the results of a price modelling, while the third subsection demonstrates the control strategy performance. The data used in this study include market prices for the summer months (December, January, and February) in Queensland, Australia, for the period from 2012 to 2018. Energy prices in this dataset show high volatility and accordingly represent a very good test case for the proposed control strategy. For load modelling, the data are provided by Western Power [36]. One hundred and twenty five selected houses were monitored from October 2012 to March 2013. Each of the 125 houses was equipped with a smart meter. The dataset provided includes the net load (which combines demand and PV generation), PV generation only, and total reactive power.

The simulation parameters are summarized in Table I.

TABLE I
Simulation Parameters

P_c (kW)	E_c (kWh)	E_{res} (kWh)	E_{end} (kWh)	α	ΔT (hour)	λ
5	10	2	5	0.96	0.5	1×10^{-3}

A. Expectation Model: ARIMA

To calculate the mathematical expectation of the future price $\mathbb{E}_{u_{k|t}}\{\bar{M}\}=\hat{\bar{M}}_{k|t},\ \forall k\in(2,H)$, a periodic ARIMA model is used as the prediction model. This model integrates the ARIMA parameters (p,d,q) with periodic autoregressive (AR), and periodic moving average (MA) models. Model orders are (3, 1, 7). The periodicity s is 48 samples (24 hours). Based on the number of outliers and total number of samples, it follows that the ratio $\gamma=0.0853$, which represents the probability that the price derives from an $\tilde{M}$ cluster.

B. Expectation Model: Mixture Model

To model the price volatility, the AEMO historical data [36] during the summer months (December, January, and February) in Queensland from 2012 to 2018 are used. The data are aggregated over a 24-hour period with a 30-min sampling interval. Figure 2 shows the price variation for aggregate data. There are 252 data samples in each time slot. The data for each 30-min interval are modelled using a mixture model (27), which yielded 47 mixture models. Note that for Fig. 2, the different colored dots are just the indicators for energy price.

Through the BIC, it appears that the number of mixture components is approximately the same for each time slot and subsequently $K=7$. Once the mixture model parameters $(\alpha_k,\mu_k,\sigma_k)$ are estimated, the mathematical expectation $\mathbb{E}_{u_{k|t}}\{\tilde{M}\}=\hat{\tilde{M}}_{k|t},\ \forall k\in(1,H)$, which includes the market price volatility, could be calculated using (28). The calculated expected value is multiplied by γ, which is the mixture coefficient in (18).

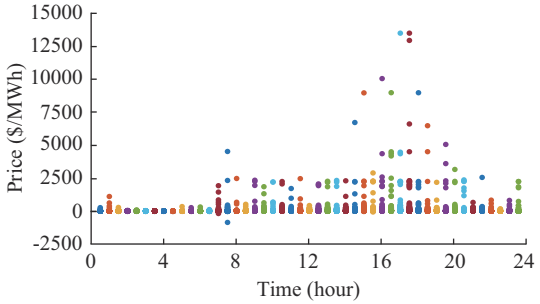

Fig. 2. Price variation for aggregate data.

The parameters of estimated mixture model for off-peak (10:00 a.m.) and peak (05:30 p.m.) hours are listed in Tables II and III, respectively. Some anomalies could be observed in the estimated mixture model, particularly for the standard deviation and mixture component probabilities. The estimated standard deviation is found to be the most sensitive to the dataset size. For future research, instead of using the approach based on expectation maximization, it is possible to use Bayesian-based inference.

TABLE II
Parameters of Estimated Mixture Model at 10:00 a.m.

α	μ	σ
0.2722	31.4	46.30
0.0078	701.1	200.50
0.0079	2230.6	0.09
0.5107	52.9	14.40
0.0118	165.1	415.70
0.1812	61.1	224.30
0.0084	465.1	8789.10

TABLE III
Parameters of Estimated Mixture Model at 05:30 p.m.

α	μ	σ
0.7547	52.3	156.400
0.0039	6625.7	0.001
0.0039	4523.2	0.001
0.0651	323.1	22155.100
0.0079	13224.5	75350.200
0.1206	132.2	2074.400
0.0439	2093.5	32594.400

C. Battery Control

To illustrate the performance of the proposed control strategy, the dynamical behavior of BESS is tested in three cases. In the first case, the market price is spike free, whereas in the second case, a market price spike of 350 \$/MWh occurs at 06: 00 p. m. The third case is the controller response for the market price spike occurring at different time during the day. Finally, a comparative study is conducted to illustrate the advantages of the progressive MPC over the conventional MPC. Regarding the net load, from the Western Power data for a house labeled 31, the daily consump-

tion on November 19, 2012 was used as a test case.

An instantaneous daily market price on December 19, 2012 and the expected values of the market price are shown in Fig. 3, where $E\{\bar{M}_t\}$ is the results of ARIMA-based price expectation; $E\{\tilde{M}_t\}$ is the the mixture model based expected values of the market price spike; and $E\{\bar{M}_t\}+E\{\tilde{M}_t\}$ is the total expected market price. Figure 4 shows the L_t, u_t, F_t, and $E(L_t)$ when there is no market price spike, where $E(L_t)$ is the average daily load used as the predicted load values.

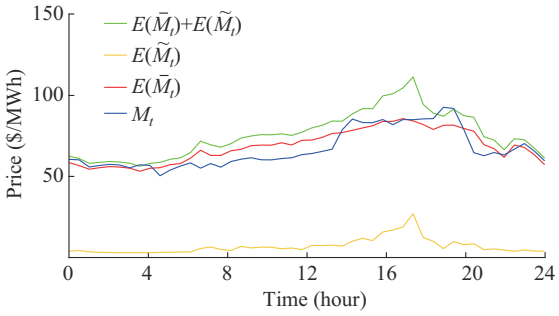

Fig. 3. Instantaneous daily market price.

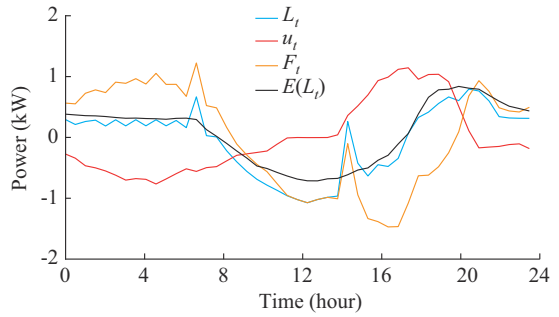

Fig. 4. L_t, u_t, F_t, and $E(L_t)$ when there is no market price spike.

The behavior of the battery power over the 24 hours changes since the battery dynamic behavior depends on the changes to the market price and net load. In the morning, the market price is low, and pMPC decides to charge the battery. At mid-day, the battery control action is constrained by the market price and the PV generation. Since the market price at mid-day is in a transition from the low value in the morning toward the high value in the afternoon, pMPC has a neutral position regarding battery charging/discharging. The battery energy when there is no market price spike is shown in Fig. 5.

Figure 5 shows that the battery is charged quickly in the morning because of the low market price. As mid-day approaches, the battery energy charges at a lower rate until it is fully charged since the market price begins to increase. Because $E(\bar{M}_t)$ in Fig. 3 begins to increase, particularly from 03:30 p.m. to 05:30 p.m., the control action of pMPC begins discharging the battery to benefit from the expected value of market price spike. Once the expected peak of the market price passes after 05:30 p.m., pMPC stops commanding rapid discharging until the predicted market price spike starts, indicating a market price drop at 07:30 p.m.. The charging process begins again after 09:00 p.m. because the battery energy needs to reach the level of the commanded 50% of the total energy capacity at midnight.

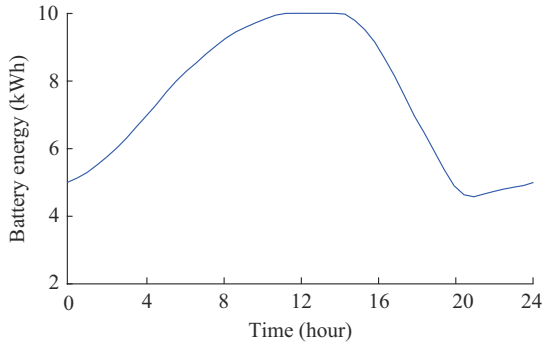

Fig. 5. Battery energy when there is no market price spike.

In the second case, at 06:00 p.m., a market price spike of 350 $/MWh occurs, as shown in Fig. 6. A comparison of the pMPC behaviors at 05:30 p.m. of these two cases reveals that the control actions and system behaviors are identical in both cases. Because we could not predict the market price spike, the difference between these two cases occurs when a market price spike occurs at 06:00 p.m., as shown in Fig. 6.

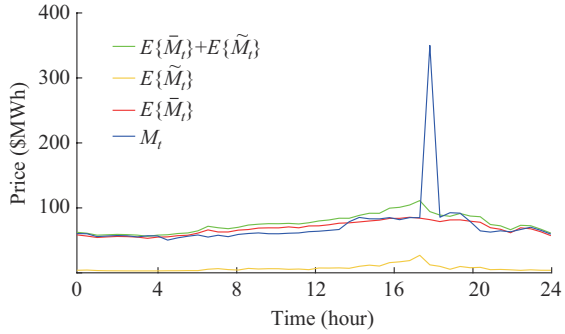

Fig. 6. Instantaneous daily market price with a market price spike and expected values of market price.

The immediate response of pMPC is to discharge the battery to respond to the market price spike, as shown in Fig. 7. As a result of battery discharging, the total energy stored in the batteries is reduced but remains above the contracted reserve, as shown in Fig. 8. For comparison, the dashed line in Fig. 8 represents the battery energy when there is no market price spike. The difference between the levels of discharged energy in the two cases is the area between the curves.

Figure 9 shows the household battery energy for multiple market price spikes during a day: 06:00 a.m., 04:00 p.m., 05:00 p.m., 06:00 p.m., and 08:00 p.m. with the same value of 350 $/MWh. Daily revenues for market price spike occurring at different time instances are summarized in Table IV.

Based on the comparison of the effects of a spike on the BESS, it follows that the proposed control strategy provides this type of response in which, regardless of the spike occurrence, the constraints are always satisfied. In other words, the battery energy neither exceeds the maximum capacity nor falls below the contracted reserve. In addition, at the end

of the prediction horizon, the battery energy is always 50% of the total energy capacity.

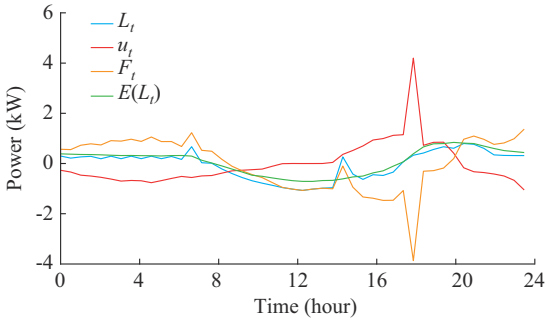

Fig. 7. L_t, u_t, F_t, and $E(L_t)$ for an immediate response of pMPC.

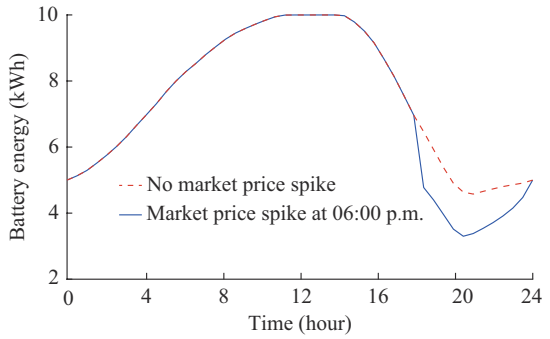

Fig. 8. Battery energy when there is a market price spike.

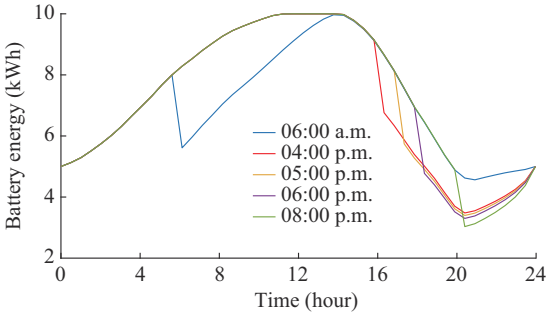

Fig. 9. Household battery energy for multiple market price spikes.

TABLE IV
DAILY REVENUE FOR MARKET PRICE SPIKE OCCURRING AT DIFFERENT TIME INSTANCES

Time instance	Revenue
06:00 a.m.	69.1
04:00 p.m.	71.7
06:00 p.m.	59.3
08:00 p.m.	55.1

The advantages of the progressive and conventional MPC-predicted control sequences are illustrated in Figs. 10 and 11, respectively. Note that the analysis focuses on the dynamic characteristics of $u_{1|t}$ and complete prediction $u_{k|t}$ on the variable horizon $k \in (1, H)$. Other colored dots in Figs. 10 and 11 present just a hint of different dynamics of control signal for different length of horizon, so that the notations are not provided. The comparison of the proposed and conventional MPC methods reveals a couple of significant differences. Unlike in the fixed-length horizon case, the equality terminal constraint on the variable-length horizon could be achieved for a daily cycling load. Toward the end of a day at $H = 48$ hours, the proposed control strategy enables the correction of BESS energy level to ensure that $E_{t_H} = E_{end}$. By contrast, when approaching the end of a day, a conventional MPC reduces the control signal to zero, making it impossible to control the BESS energy level at the end of the day. The most notable difference is related to the optimality of the solution. Unlike a conventional MPC, the proposed control strategy achieves high power levels during charging and discharging in the fully charged BESS. The importance of the global optimality property of the proposed control strategy is reflected in the execution time of the program. Although the algorithm is implemented in MATLAB, we observe a significant difference in the computational time. The proposed control strategy is executed for approximately 21 s, whereas the conventional MPC requires approximately 145 s.

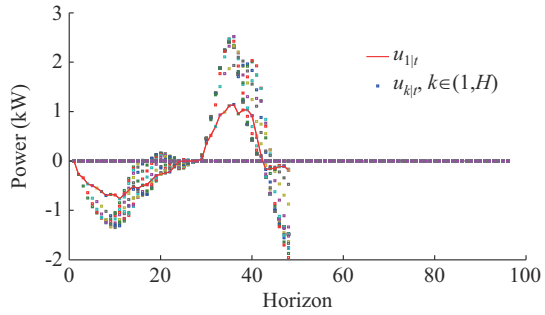

Fig. 10. Progressive MPC-predicted control sequence.

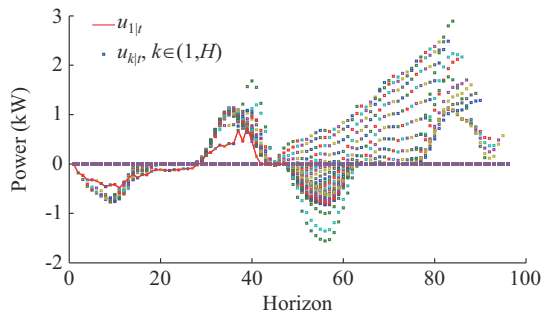

Fig. 11. Conventional MPC-predicted control sequence.

The results illustrate the fundamental characteristics of the proposed method. It remains to be demonstrated how the proposed method performs better than the conventional MPC method. For this purpose, 200 realizations, each with a 24-hour duration, are used for the evaluation. Each of these realizations for market price and net load is tested for both cMPC and pMPC. Total daily income is calculated, where histograms of total daily income for cMPC and pMPC are given in Fig. 12, where the orange and green lines are the probability density curves of cMPC and pMPC, respectively. It can be observed that pMPC ($\mu_{pMPC} = 11.57$) has a substantially higher income as compared with that of cMPC ($\mu_{cMPC} =$

1.38). The estimated standard deviation is similar for the two cases with $\sigma_{pMPC}=1.76$ and $\sigma_{cMPC}=1.93$.

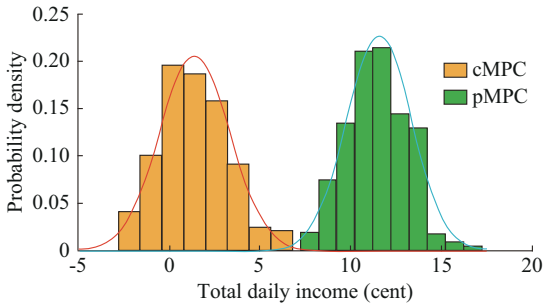

Fig. 12. Total daily income for cMPC and pMPC.

VI. Conclusion

The investment in BESSs for residential customers may provide significant economic benefits. This is valid only if the applied control strategy is capable of managing associated volatility. Since the market price and daily cycling net load contribute the most to unpredictable behavior, this paper models and quantifies their probabilistic nature by mathematical expectation. The expected market price consists of the predicted base price and the expected value of market price spikes. Using a mixture model to compute the expected value of market price spikes is shown to be a simple and effective approach. The proposed control strategy is based on a new convex cost function that depends on the expected values of the market price and daily cycling net load. The cost function is optimized on the variable-length horizon to accommodate the repetitive behavior of the customer net load. The use of variable horizon length enables the equality terminal condition to be defined, which is one of the requirements of global optimality with the proposed methodology. The proposed approach is tested on real market and customer load data. The approach demonstrates superior performance, generating a significantly higher income compared with the conventional MPC. This performance is a result of including the expected value of market price spikes in the cost function as well as the variable-length horizon.

The future work will focus on developing a control strategy for customer battery storage in the case of neighborhood energy trading. This will require an extension of the probabilistic model as well as a broader application of data-driven methods for probability density modelling.

References

[1] U. Damisa, N. I. Nwulu, and Y. Sun, "Microgrid energy and reserve management incorporating prosumer behind-the-meter resources," *IET Renewable Power Generation*, vol. 12, no. 8, pp. 910-919, Aug. 2018.

[2] D. Wu, M. Kintner-Meyer, T. Yang *et al*., "Economic analysis and optimal sizing for behind-the-meter battery storage," in *Proceedings of 2016 IEEE PES General Meeting*, Boston, USA, Jul. 2016, pp. 1-5.

[3] S. J. Rassenti, V. L. Smith, and B. J. Wilson, "Controlling market power and price spikes in electricity networks: demand-side bidding," *Proceedings of the National Academy of Sciences*, vol. 100, no. 5, pp. 2998-3003, May 2003.

[4] H. Manner, D. Tűrk, and M. Eichler, "Modeling and forecasting multivariate electricity price spikes," *Energy Economics*, vol. 60, pp. 255-265, Jan. 2016.

[5] A. Nazarova, "Stochastic models for energy markets: statistics, pricing and model risk," Ph. D. dissertation, der Fakultt fűr Mathematik der Universitä.

[6] A. Eydeland and K. Wolyniec, *Energy and Power Risk Management New Developments in Modeling, Pricing, and Hedging*. Hoboken: Wiley, 2003.

[7] R. H. Byrne and C. A. Silva-Monroy, "Estimating the maximum potential revenue for grid connected electricity storage: arbitralge and regulation," Sandia National Laboratories, Tech. Rep. Jan. 2012.

[8] J. Situ and D. Wright, "Economic analysis of commercial PV microgrids," in *Proceedings of 2017 IEEE International Conference on Smart Energy Grid Engineering (SEGE)*, Oshawa, Canada, Aug. 2017, pp. 110-116.

[9] B. Tudu, K. K. Mandal, and N. Chakraborty, "Behind the meter optimization of grid connected PV system," in *Proceedings of 2018 International Conference on Computing, Power and Communication Technologies (GUCON)*, New Delhi, India, Sept. 2018, pp. 500-503.

[10] E. Camacho and C. Bordons, *Model Predictive Control*. London: Springer, 2007.

[11] A. Mahamadi and S. Sastry, "Model predictive controller for battery management systems," in *Proceedings of 2015 International Conference on Computing, Control, Networking, Electronics and Embedded Systems Engineering (ICCNEEE)*, Khartoum, Sudan, Sept. 2015, pp. 21-26,.

[12] T. G. Paul, S. J. Hossain, S. Ghosh *et al*., "A quadratic programming based optimal power and battery dispatch for grid-connected microgrid," *IEEE Transactions on Industry Applications*, vol. 54, no. 2, pp. 1793-1805, Mar. 2018.

[13] S. Teleke, M. E. Baran, S. Bhattacharya *et al*., "Rule-based control of battery energy storage for dispatching intermittent renewable sources," *IEEE Transactions on Sustainable Energy*, vol. 1, no. 3, pp. 117-124, Oct. 2010.

[14] J. Lee, P. Zhang, L. Gan *et al*., "Optimal operation of an energy management system using model predictive control and Gaussian process time-series modeling," *IEEE Journal of Emerging and Selected Topics in Power Electronics*, vol. 6, pp. 1783-1795, Dec. 2018.

[15] K. Worthmann, C. M. Kellett, P. Braun *et al*., "Distributed and decentralized control of residential energy systems incorporating battery storage," *IEEE Transactions on Smart Grid*, vol. 6, no. 4, pp. 1914-1923, Jul. 2015.

[16] Z. Yu, L. Jia, M. C. Murphy-Hoye *et al*., "Modeling and stochastic control for home energy management," *IEEE Transactions on Smart Grid*, vol. 4, no. 4, pp. 2244-2255, Dec. 2013.

[17] C. Zhang, J. Wu, Y. Zhou *et al*., "Peer-to-peer energy trading in a microgrid," *Applied Energy*, vol. 220, pp. 1-12, Jan. 2018.

[18] D. P. Jovanović, G. F. Ledwich, and G. R. Walker, "Electricity tariff aware model predictive controller for customer battery storage with uncertain daily cycling load," *Journal of Modern Power Systems and Clean Energy*, vol. 10, no. 1, pp. 140-148, Jan. 2022.

[19] J. B. Copetti, E. Lorenzo, and F. Chenlo, "A general battery model for PV system simulation," *Progress in Photovoltaics: Research and Applications*, vol. 1, no. 4, pp. 283-292, Apr. 1993.

[20] J. F. Manwell and J. G. McGowan, "Extension of the kinetic battery model for wind/hybrid power systems," *Proceedings of EWEC*, vol. 3, pp. 284-289, Mar. 1994.

[21] O. Tremblay and L. A. Dessaint, "Experimental validation of a battery dynamic model for EV applications," *World Electric Vehicle Journal*, vol. 3, no. 2, pp. 289-298, Feb. 2009.

[22] S. Boyd and L. Vandenberghe, *Convex Optimization*. Cambridge: Cambridge University Press, 2004.

[23] W. R. Wade, "The bounded convergence theorem," *The American Mathematical Monthly*, vol. 81, no. 4, pp. 387-389, Apr. 1974.

[24] J. Gruber, S. Jahromizadeh, M. Prodanović *et al*., "Application-oriented modelling of domestic energy demand," *International Journal of Electrical Power & Energy Systems*, vol. 61, pp. 656-664, May 2014.

[25] S. Borovkova and M. D. Schmeck, "Electricity price modeling with stochastic time change," *Energy Economics*, vol. 63, pp. 51-65, Jan. 2017.

[26] F. E. Benth, J. Kallsen, and T. Meyer-Brandis, "A non-Gaussian Ornstein-Uhlenbeck process for electricity spot price modeling and derivatives pricing," *Applied Mathematical Finance*, vol. 14, no. 2, pp. 153-169, Feb. 2007.

[27] B. Jiang, J. Pei, Y. Tao *et al*., "Clustering uncertain data based on probability distribution similarity," *IEEE Transactions on Knowledge and Data Engineering*, vol. 25, pp. 751-763, Apr. 2013.

[28] G. McLachlan and D. Peel, *Finite Mixture Models*. New York: Wiley, 2000.

[29] S. Leorato, "A refined Jensen's inequality in Hilbert spaces and empir-

ical approximations," *Journal of Multivariate Analysis*, vol. 100, no. 5, pp. 1044-1060, May 2009.
[30] G. Grimmett and D. Stirzaker, *Probability and Random Processes*. Oxford: Oxford University Press, 2008.
[31] C. Robert and G. Casella, *Monte Carlo Statistical Methods*, New York: Springer-Verlag, 2004.
[32] G. E. P. Box, G. M. Jenkins, and G. C. Reinsel, *Time Series Analysis: Forecasting and Control*. New Jercy: Prentice Hall, 1994.
[33] V. Barnett and T. Lewis, *Outliers in Statistical Data*. New York: Wiley & Sons, 1994.
[34] J. Lago, F. D. Ridder, and B. D. Schutter, "Forecasting spot electricity prices: deep learning approaches and empirical comparison of traditional algorithms," *Applied Energy*, vol. 221, pp. 386-405, Feb. 2018.
[35] P. H. Franses and R. Paap, *Periodic Time Series Models*. Oxford: Oxford University Press, 2004.
[36] Western Power. (2019, Jan.). [Online]. Available: https://westernpower.com.au/
[37] Australian Energy Market Operator. (2019, Jan.). [Online]. Available: https://www.aemo.com.au/

Dejan P. Jovanović received the B.Sc. degree in electrical and microelectronic engineering and the M. Sc. degree in systems control engineering from the University of Belgrade, Belgrade, Serbia, in 1996 and 2002, respectively, and the Ph. D. degree in statistics from the University of Queensland, Brisbane, Australia, in 2014. He has held different positions both in industry and academia. His research interests include control system, power electronics, and application of machine learning in fault diagnosis and fault-tolerant control.

Gerard F. Ledwich received the Ph. D. degree in electrical engineering from the University of Newcastle, Newcastle, Australia, in 1976. He is currently a Research Professor of electric power with the School of Electrical Engineering and Robotics, Queensland University of Technology, Brisbane, Australia. He has 215 journal publications and 323 refereed conference publications. He has a Scopus H-index of 44, and a citation count of 8633. He has been involved in securing grants of more than AU$16 million, with the majority of them were in explicit partnership with industry. His research interests include power system, power electronics, and wide-area control of smart grid.

Geoffrey R. Walker received the B.E. and Ph.D. degrees from The University of Queensland, Brisbane, Australia, in 1990 and 1999, respectively. From 1998 to 2007, he was the Power Electronics Lecturer with The University of Queensland. From 2008 to 2013, he was a Senior Electrical Engineering Consultant with Aurecon's Transmission and Distribution Group, Brisbane, across various areas including rail traction, grounding studies, electricity transmission planning, and renewable energy project design and review. In 2013, he joined the Electrical Power Engineering Group, Queensland University of Technology, Brisbane, as an Associate Professor. His current research interests include applying power electronics to applications in renewable energy (especially photovoltaic), power system, and electric vehicle.